

**Determination of Oxygen in Zircaloy
Surfaces by Means of Charged Particle
Activation Analysis**

J. Lorenzen and D. Brune

This report is intended for publication in a periodical. References may not be published prior to such publication without the consent of the author.



AKTIEBOLAGET ATOMENERGI

STUDSVIK, NYKÖPING, SWEDEN 1972

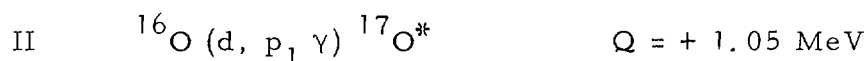
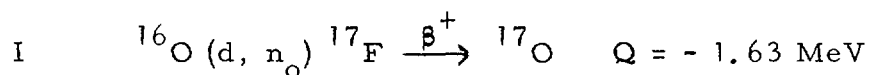
Determination of Oxygen in Zircaloy Surfaces by Means of Charged
Particle Activation Analysis

J Lorenzen and D Brune

AB Atomenergi, Studsvik, Sweden

SUMMARY

Oxygen in zircaloy surfaces has been determined by means of charged particle activation analysis employing the following two reactions



The detection limits for oxygen in such surfaces has been investigated by measuring the promptly emitted 0.87 MeV gamma rays (reaction II) and also the 511 keV annihilation radiation which arises from β^+ -decay of ${}^{17}\text{F}$ (reaction I). The correlation between the detection limit for oxygen in zircaloy, the particle energy and the surface thickness analyzed has been evaluated.

At a deuteron energy of 3 MeV a detection limit of $0.7 \cdot 10^{-7} \text{ g/cm}^2$ was obtained from the measurement of the prompt gamma radiation arising from the second of these reactions.

The analysis carried out by means of this technique is characterized by a high degree of rapidity.

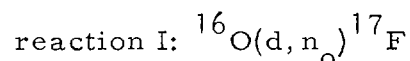
INTRODUCTION

Charged particle activation analysis of light elements such as carbon, nitrogen and oxygen in metal surfaces has been studied previously by various investigators [1 - 3]. This form of analysis permits determination of either the integral content of the light element in the surface [e. g. 1] or the concentration profile of the light element below the surface [e. g. 2, 3]. Usually, the excitation functions for (d,n)- and (d,p)-reactions for various light elements increase with particle energies up to a few MeV [4, 5]. This implies an improved detection limit for the element in the surface with increasing particle energy. It should be noted, however, that the penetration depth of the particle also increases so that a thicker surface layer is involved.

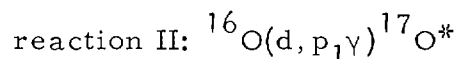
REACTIONS AND MEASUREMENT

In the present study the correlation between particle energy, thickness of layer at the surface and detection limit of oxygen in zircaloy was considered for the reactions mentioned below.

In the context of these two reactions oxygen can be identified by



- 1) Neutron time-of-flight measurement [3]
- 2) Measurement of the induced β^+ -activity from ^{17}F ($T_{1/2} = 66$ sec)



- 3) Proton spectroscopy [6]
- 4) Measurement of prompt 0.87 MeV- γ -radiation

The present work makes use of techniques 2) and 4).

APPLICATION OF THE PRINCIPLE OF CONVOLUTION TO
SURFACE ANALYSIS

Proton induced reactions often exhibit sharp resonances in the reaction cross section. These resonances can be used for the depth determination of the light elements in the stopping matter [2]. For deuteron induced reactions, however, the cross section alters very little with energy. Accordingly, the yield corresponds approximately to bulk contribution from the whole range interval. Along the range the deuteron energy decreases continuously and a specific depth corresponds to a certain energy, i. e. to a certain value in the excitation function. There is accordingly a relationship between the depth and the reaction cross section. Furthermore, the yield from any part of the range is determined by the product of the nuclei density and the reaction cross section corresponding to this depth. Thus the convolution integral over the cross section and the depth will give the activity induced over the different ranges corresponding to different particle energies. The approach can be understood in the following terms.

The activity $A(\Delta x)$ induced within the depth Δx corresponding to the energy interval from E_d to $E_d - \Delta E$ (energy decrease caused by the stopping power of the material) is given by

$$A(\Delta x) = K \cdot N(\Delta x) \cdot I_d \cdot \bar{\sigma}(E_d, \Delta E) \cdot \Omega \cdot \eta \cdot R^{-2}$$

where

- K = proportionality constant
- $N(\Delta x)$ = amount of target nuclei within the interval Δx . Δx is defined by the deuteron energies E_d and $(E_d - \Delta E)$
- I_d = deuteron current density
- $\bar{\sigma}(E_d, \Delta E)$ = mean cross section between E_d and $(E_d - \Delta E)$
- Ω = solid angle (detector)
- R = distance between radiation source and detector
- η = detector efficiency

The measured radiation is produced by activation within the effective range R_{eff} of the charged particle. Thus $R_{\text{eff}}(E) = R(E) - R(E_{\text{thresh}})$ since at a depth $R > R_{\text{eff}}$ no reaction can occur for $E_d < E_{\text{thresh}}$.

Accordingly the convolution integral can be written

$$A(R_{\text{eff}}) = \int_0^{R_{\text{eff}}} A(x) dx = K \cdot I_d \cdot \Omega \cdot \eta \cdot R^{-2} \int_{E_{d,0}}^{E_{\text{thresh}}} \sigma(E) \cdot N(x) dE$$

$N(x)$ is included under the integral since x is related to E_d by the stopping power $(dE/dx)_{\text{matrix}}$. The relationship $R_{\text{eff}} = \sum_i^M \Delta x_i$ permits numerical integration according to the expression

$$A(R_{\text{eff}}) = C \cdot \sum_i \left\{ \sigma_i \cdot N_i \cdot \Delta E_i \right\}$$

where

$$C = K \cdot I_d \cdot \Omega \cdot \eta \cdot R^{-2}$$

σ_i = mean cross section over the energy interval $(dE/dx)_i \cdot \Delta x_i$

N_i = number of target nuclei within range Δx_i

If the sample is homogeneous with respect to the distribution of target nuclei, N_i is a constant and can be separated as follows

$$A(R_{\text{eff}}) = C \cdot N \cdot \sum_i \left\{ \sigma_i \cdot (dE/dx)_i \cdot \Delta x_i \right\}$$

This is the formula which was used to calculate the expected activity distribution with energy. In Fig 2 the theoretical values obtained are normalized to the experimental points since K is unknown.

ESCAPE OF NUCLIDES FROM THE IRRADIATED SURFACE
DUE TO THE RECOIL EFFECT

In accordance with the kinetics of nuclear reactions a nuclide formed in the metal surface acquires a certain amount of kinetic energy and may in consequence escape from this surface.

As regards reaction I, the conservation of momentum gives

$$\bar{P}_d + \bar{P}_{16\text{O}} = \bar{P}_{17\text{F}} + \bar{P}_n$$

Since ^{16}O is at rest this reduces to

$$\bar{P}_{17\text{F}} = \bar{P}_d - \bar{P}_n$$

Numerical calculations show that $\bar{P}_{17\text{F}} > 0$. Thus the ^{17}F nucleus always moves into the sample as the deuteron and therefore cannot escape from the target. Thus no activity can be lost.

Similarly, consideration of reaction II leads to

$$\bar{P}_{17\text{O}} = \bar{P}_d - \bar{P}_p$$

In this reaction, Q has a positive value, and a negative value of $\bar{P}_{17\text{O}}$ is therefore possible. Since, however, the measurement is based on prompt gamma radiation, lack of activity due to the recoil effect will not be experienced even when Q is positive. Although the recoil effect has no influence on the yield in this particular instance, there are other reactions which may be of interest where the loss of decaying nuclei can become significant. Thus for all exoergic reactions this effect should be considered.

EXPERIMENTAL

Accelerator and measurements

The 5.5 MeV Van de Graaff accelerator at AB Atomenergi, Studsvik, was used as the irradiation facility. In this device a DC deuteron beam is produced at energies between 0.9 and 5.5 MeV. The beam is focussed by two pairs of quadrupole lenses and defined on the target by collimators of tantalum with holes between 1.2 and 0.6 cm, located at the terminal section of the tube.

The gamma radiation induced in the samples was detected by a 3" x 3" NaI (Tl) crystal and after selection in a discriminator the spectrum was fed into a 16 x 256-channel multichannel analyzer (MCA) of Nuclear Data type.

In order to avoid thermal defects in the sample only currents of the order of 0.5 μ A were used [2]. The target holder is isolated from the rest of the tube so that the total charge can be collected. This was recorded in an ELCOR-current integrator.

During the period of irradiation (60 sec) both prompt gamma radiation and annihilation quanta were detected. Immediately after completion of the irradiation the decay was measured during a series of 10 sec intervals. The annihilation quanta produced in each period were recorded using one of the 16 subgroups in the MCA. The radiation background was measured before and after each series and account was taken of both time-dependent and time-independent backgrounds.

Samples

Three different kinds of sample were used. ZrO_2 and a sample of oxidized metallic Zr (~ 800 ppm O_2) were used for the oxygen determination while a sample of pure zirconium metal served as a back-

ground reference. All the samples were cleaned in acetone before irradiation and mounted together on a multi-specimen sample changer. This technique allowed the samples to be kept in vacuum throughout the experiment.

Analysis

The gamma-ray spectra measured were analyzed with the aid of an 8 K-PDP 15 digital computer. The peaks were corrected for background and normalized with respect to lifetime (channel 0) and charge. Because of the very different activities of oxygen-rich and oxygen-poor samples it was necessary to adjust the distance between detector and source for each group of measurements to afford a reasonable dead-time. The activity was subsequently normalized to a detector distance of 32 cm.

The irradiation was carried out at three deuteron energies, namely 2.3, 2.6 and 3.0 MeV.

RESULT AND DISCUSSION

The reactions $^{16}\text{O}(d, n_0)^{17}\text{F}$ and $^{16}\text{O}(d, p_1\gamma)^{17}\text{O}^*$ can be used to determine the concentration of oxygen in zirconium or zircaloy. According to the graph in Fig 2 performance of the analysis by prompt gamma ray measurements is associated with the lowest detection limit i. e. $(0.70 \pm 0.01) \cdot 10^{-7}$ g/cm² or (10.0 ± 0.1) ppm oxygen in zircaloy considering an irradiation period of 1 min. This can be understood as a consequence of the greater activation depth in comparison with that of the $^{16}\text{O}(d, n_0)^{17}\text{F}$ reaction. The detection limit is defined as the amount of oxygen giving rise to a signal which is three times greater than the background variation. The variation is calculated as the square root of the background counts from all those channels that define the width of the peak.

In general it is possible to calculate the expected activity through the principle of convolution. Since, however, the errors in the measured values of the reaction cross-sections are still of the order of 20 - 30 % this type of result requires careful handling [5, 9].

Since the excitation function increases with energy, [Fig 1], activity is expected to follow suit. This can be seen in Fig 2. Thus, although the efficiency of the NaI(Tl) crystal is lower for 870 keV gamma rays than for the 511 keV quanta the prompt activity is much higher. This is accounted for in terms of the higher cross-section for $^{16}\text{O}(d, p_1 \gamma) ^{17}\text{O}^*$ and the positive Q-value of this reaction. Since the negative Q-value in $^{16}\text{O}(d, n_0) ^{17}\text{F}$ is responsible for the much smaller value of R_{eff} , activation is produced in a smaller zone by (d, n) than by (d, p) for a given energy (see Table 1) [$\sigma(d, p) \approx 0$ below 400 keV]

Table 1 [7]

E_d (MeV)	R_d (μm)	$R_{\text{eff}}(d, p)$ (μm)	$R_{\text{eff}}(d, n)$ (μm)
2.3	25	21	7
2.6	30	26	12
3.0	37	34	19

Correlation: particle energy – effective range in zircaloy

Electrical conductivity is dependent on the concentration of oxygen in a metal and decreases with the oxygen content. Care must therefore be exercised with recordings of current when oxygen-rich samples are run. The reliability of the current recording increases as the concentration of oxygen in the metal falls. In the present instance the recording from the current integrator was compared with the measured current from a tantalum plate which was inserted in the beam from time to time.

It is worth mentioning that the atomic number of the matrix has a considerable influence on the detection limit of oxygen. Since zirconium has a rather high value of Z compared with that of oxygen the signal to background ratio is quite good. The determination of oxygen in alloys such as steel is much more difficult to accomplish, essentially due to the lower value of Z for iron which causes an increase in background radiation [see Table 2].

A comparison of the two methods used in this investigation indicates a preference for gamma-ray measurements not merely because of the better detection limit which is attained but also in view of the shorter running time which is required. Thus the gamma peak is built up during an activation time of one minute, while it is necessary to follow the β^+ -decay curves for periods which are at least three times longer. Furthermore, the analysis in which the area of a single peak is measured (0.87 MeV) is more rapidly performed than an analysis which involves the measurement of the several peak areas necessary for characterizing the decay curve (0.51 MeV) [Fig 4].

It is expected that more than 10 analyses per hour can be achieved using the reaction $^{16}\text{O}(d, p, \gamma)^{17}\text{O}^*$ in combination with a remotely controlled sample changer.

COMPARISON WITH OTHER NUCLEAR METHODS

Various methods indicating a very high degree of sensitivity for determining oxygen in metals have been reported in the literature. Some of these methods have been collected in Table 2.

Table 2

Bombarding Particle	Energy in MeV	Notes	Detection limit	Reference
T	< 3		$10^{-3} \mu\text{g}/\text{cm}^2$	10
P	< 3	different isotopes of Oxygen	$10^{-6} \mu\text{g}/\text{cm}^2$	11
^3He , ^4He	30; 55	Oxygen in pure metals	10^{-2} ppm	12
P; ^3He	12; 15	Oxygen in silicon	10^{-3} ppm	13
P	10 - 15	Oxygen in extremely	10^{-5} ppm	14
^3He	10 - 20	pure materials	10^{-6} ppm	14
^4He	40	(Si, Fe, Nb)	10^{-6} ppm	14

Ricci and Hahn have measured the relationship between energy and sensitivity for the reaction $^{16}\text{O}(^3\text{He}, \text{p})^{18}\text{F}$ in the energy interval between 3 and 10 MeV [15]. They have also published a sensitivity list for 15 light elements (Be \rightarrow Ca) with reference to reactions initiated by 18 MeV ^3He -particles [16]. By comparison they have also measured the detection limits for oxygen in thick and thin targets bombarded with 4 - 10 MeV ^3He -particles [17].

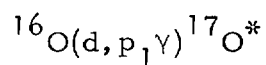
REFERENCES

1. CHEN, N.S. , and FREMLIN, J. H. ,
Determination of carbon and nitrogen by deuteron-induced
prompt gamma radiations.
Radiochem. Radioanal. Letters 4 (1970) p. 365.
2. BRUNE, D. , LORENZEN, J. , and WITALIS, E. ,
Depth distribution studies of carbon in steel surfaces by means
of charged particle activation analysis with an account of heat
and diffusion effects in the sample. 1972.
(AE-451)
3. LORENZEN, J. , and MALMSKOG, S. ,
1972. AB Atomenergi, Sweden.
(Internal report. FK-40)
4. JARMIE, N. , and SEAGRAVE, J. D. , (Ed.)
Charged particle cross sections. 1957.
(LA-2014)
- 5a. WOHLLEBEN, K. , and SCHUSTER, E. ,
Aktivierungsanalyse mit Deuteronen.
Radiochim. Acta 12 (1969) p. 75.
- 5b. WOHLLEBEN, K. , and SCHUSTER, E. ,
Der totale Wirkungsquerschnitt der Reaktion $^{12}\text{C}(d,n)^{13}\text{N}$ für
Deuteronen von 0.4 bis 3.0 MeV.
Op. cit. , 8 (1967) p. 78.
6. AMSEL, G. et al. ,
Use of the nuclear reaction $\text{O}^{16}(d,p)\text{O}^{17}$ to study oxygen diffusion
in solids and its application to zirconium.
J. Appl. Phys. 39 (1969) p. 2246.
7. WILLIAMSON, C. F. , BOUJOT, J. P. , and PICARD, J. ,
Tables of range and stopping power of chemical elements for
charged particles of energy 0.5 to 500 MeV. 1966.
(CEA-R-3042)
8. MAYER, J. W. , ERIKSSON, L. , and DAVIES, J. A. ,
Ion implantation in semiconductors:silicon and germanium.
Academic Press, New York 1970. p. 15.
9. DIETZSCH, O. et al. ,
Deuteron-induced reactions on ^{16}O .
Nucl. Phys. A 114 (1968) p. 330.
10. BARRANDON, J. N. , and ALBERT, P. ,
Contribution au dosage de l'oxygène dans les pellicules super-
ficielles par irradiation avec des tritons de 3 MeV.
Rev. Phys. Appl. 3 (1968) p. 111.
(CONF-681003, p. 794 in English)

11. AMSEL, G., and SAMUEL, D.,
Microanalysis of the stable isotopes of oxygen by means of
nuclear reactions.
Anal. Chem. 39 (1967) p. 1689
12. DEBRUN, J.-L., BARRANDON, J.N., and ALBERG, P.,
Contribution to activation analysis by charged particles; deter-
mination of carbon and oxygen in pure metals, possibilities of
sulphur determination.
Modern trends in activation analysis. Proc. of the 1968 Intern.
Conf. ... Gaithersburg, Md., 7 - 11 Oct. 1968. Ed. DeVore,
J.R. U.S. Government Printing Office, Washington, D.C., 1969.
p. 774.
(NBS Spec. Publ. 312. Vol. 2.) (CONF-681003)
13. NOZAKI, T. et al.,
Particle activation analysis of carbon, nitrogen, and oxygen in
semiconductor silicon.
Op. cit., p. 842.
14. ENGELMANN, C.,
L'analyse par activation dans les particules chargées et les
photons gamma.
Bull. Inform. Sci. Tech. (1969):140 p. 65
(ORNL-TR-2265 in English)
15. RICCI, E., and HAHN, R.L.,
Rapid calculation of sensitivities, interferences, and optimum
bombarding energies in ^3He activation analysis.
Anal. Chem. 40 (1968) p. 54.
16. RICCI, E., and HAHN, R.L.,
Sensivities for activation analysis of 15 light elements with 18-
MeV helium 3 particles.
Op. cit., 39 (1967) p. 794.
17. RICCI, E., and HAHN, R.L.,
Theory and experiment in rapid, sensitive helium-3 activation
analysis. Helium-3 reactions as neutron sources.
Op. cit., 37 (1965) p. 742.
18. AMSEL, G.,
Microanalysis of the stable isotopes of oxygen by means of nucle-
ar reactions.
Anal. Chem. 39 (1967) p. 1689.
19. AMSEL, G.,
Microanalyse par l'observation de reactions nucléaires. Applica-
tions a la physique du solide.
Thesis. 1963.
(LAL-1053)

FIGURE CAPTIONS

Fig 1. Total cross-section for the reactions:



(0.2 - 1.1 MeV) [18], (1.1 - 2.0 MeV) [4], (2.0 - 3.0 MeV) [9]

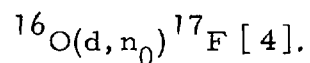


Fig 2. Curves for measured (X, O) and calculated (Δ , \square) activities referring to prompt gamma- and annihilation radiation (decay).

The energy scale shows incident deuteron energy. Effective range scales are presented for (d, n) and (d, p)-reactions, respectively.

Fig 3. Calculated detection limits obtained from the experimental values. Scales as defined in Fig 2.

Fig 4. Decay curve for the induced ^{17}F activity.

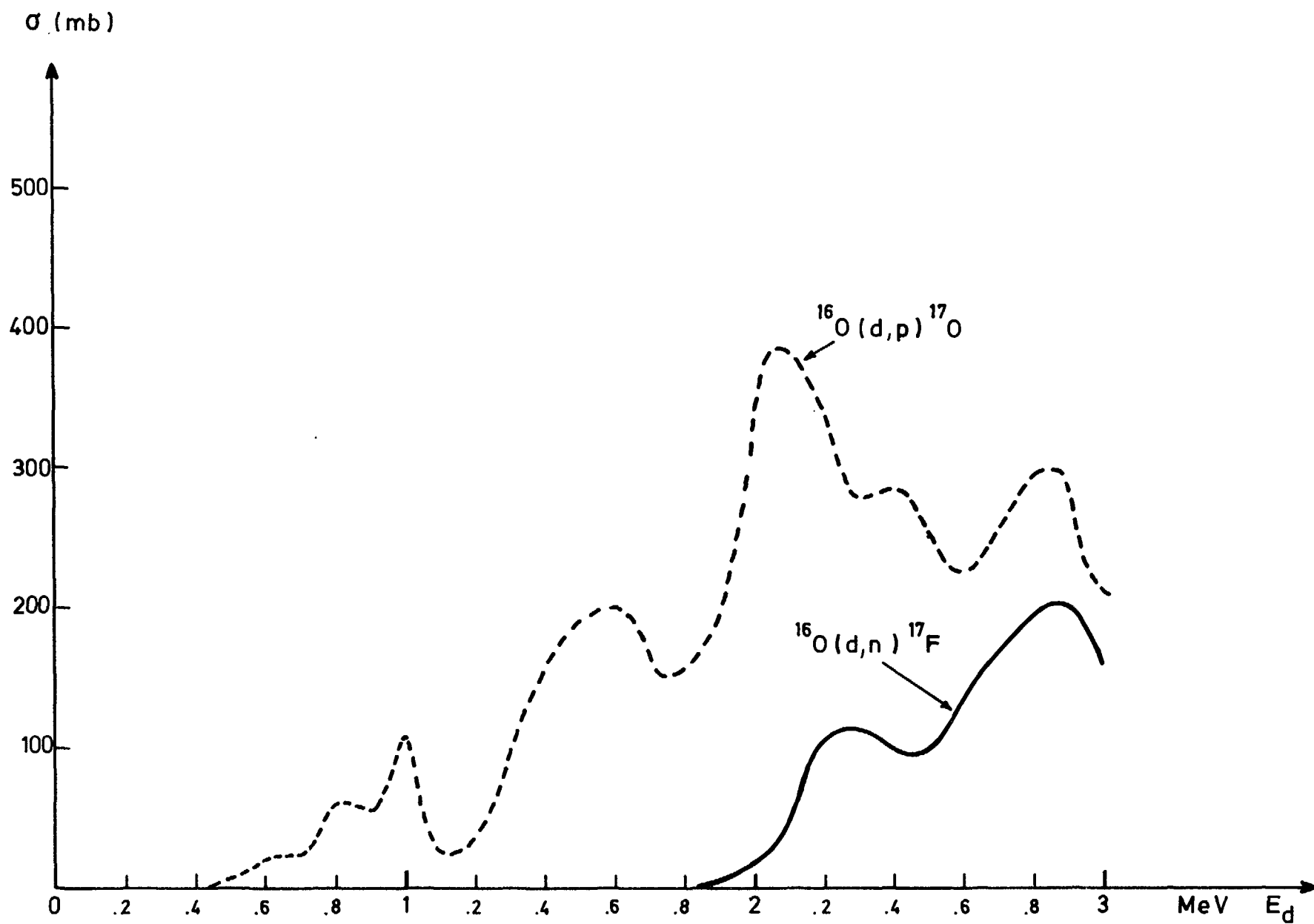


Fig. 1

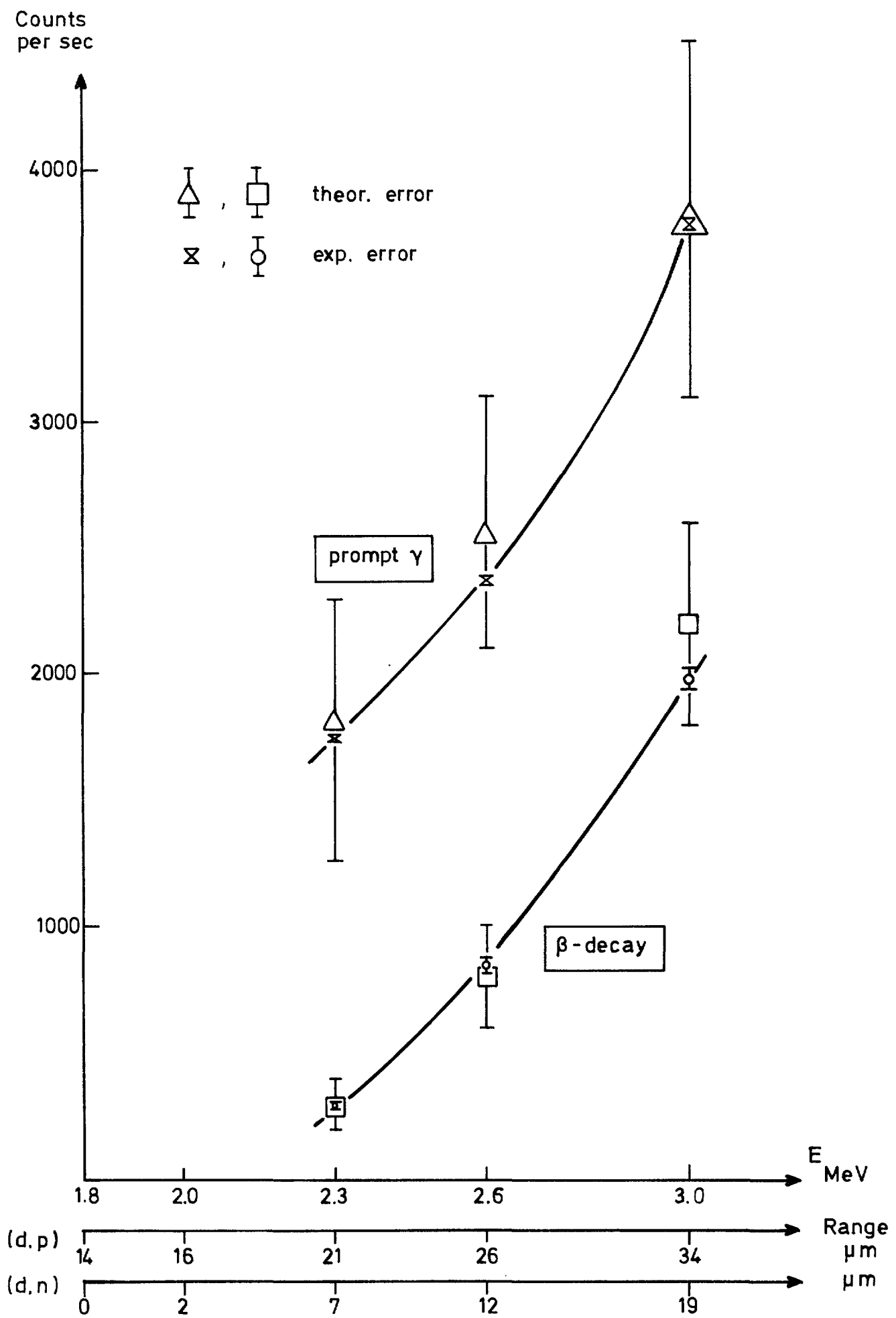


Fig. 2

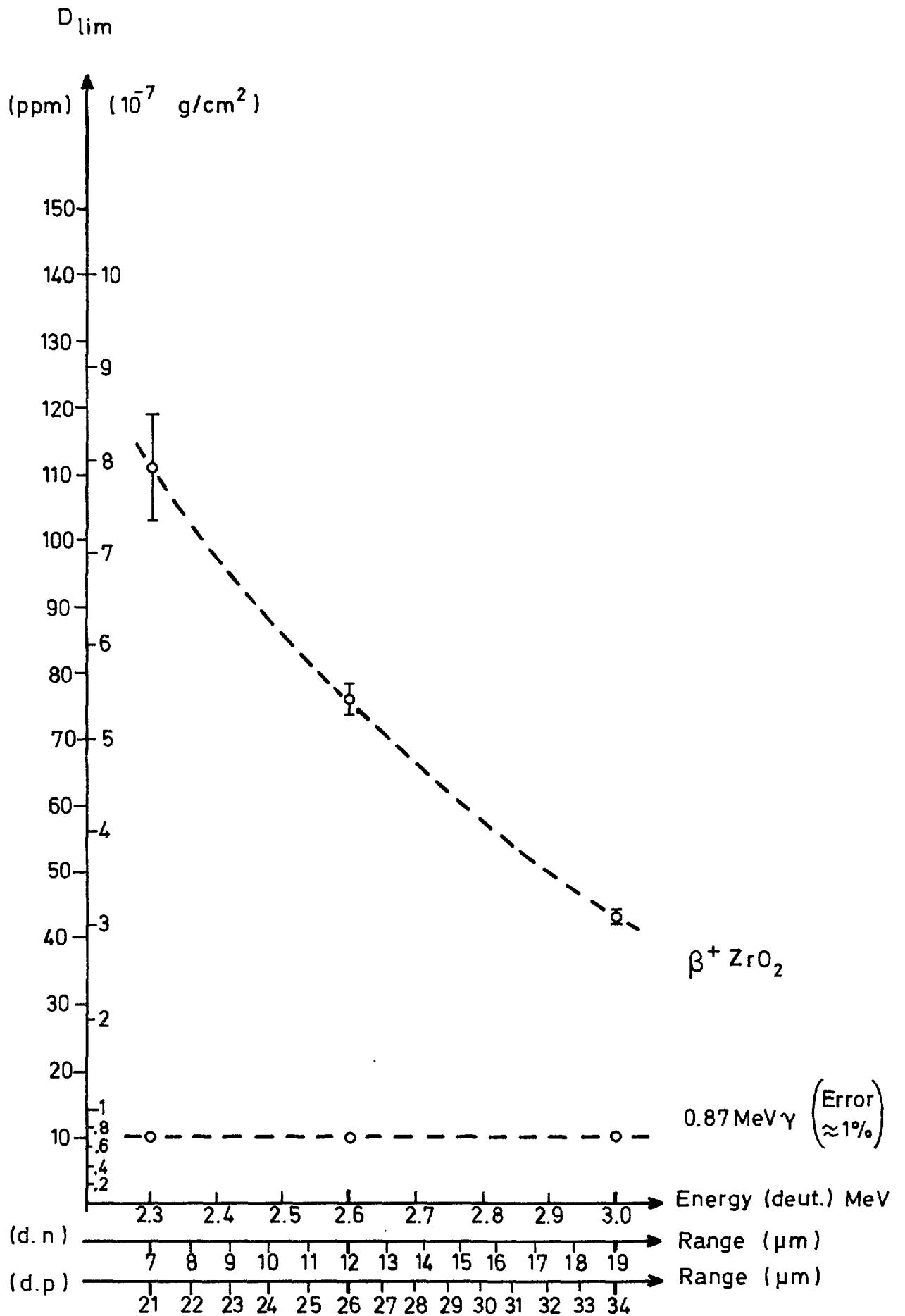


Fig. 3

Counts per 10 sec

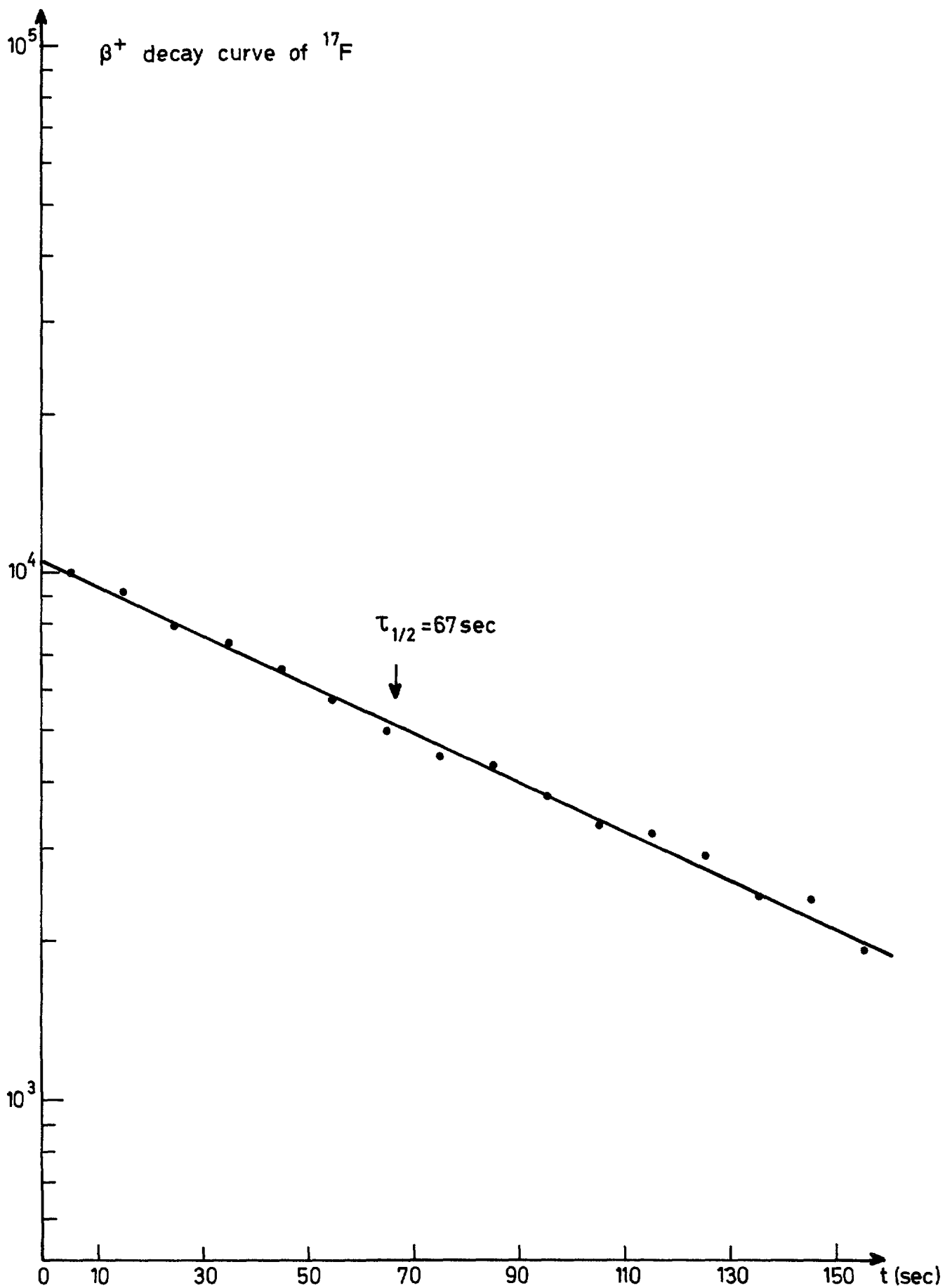


Fig. 4

LIST OF PUBLISHED AE-REPORTS

1-390 (See back cover earlier reports.)

391. Half-life measurements in ^{141}I . By V. Berg and A. Höglund. 1970. 16 p. Sw. cr. 10:--.
392. Measurement of the neutron spectra in FRO cores 5, 9 and PuB-5 using resonance sandwich detectors. By T. L. Andersson and M. N. Qazi. 1970. 30 p. Sw. cr. 10:--.
393. A gamma scanner using a Ge(Li) semi-conductor detector with the possibility of operation in anti-coincidence mode. By R. S. Forsyth and W. H. Blackadder. 1970. 22 p. Sw. cr. 10:--.
394. A study of the 190 keV transition in ^{141}La . By B. Berg, A. Höglund and B. Fogelberg. 1970. 22 p. Sw. cr. 10:--.
395. Magnetoacoustic waves and instabilities in a Hall-effect-dominated plasma. By S. Palmgren. 1970. 20 p. Sw. cr. 10:--.
396. A new boron analysis method. By J. Weitman, N. Däverhög and S. Farvolden. 1970. 26 p. Sw. cr. 10:--.
397. Progress report 1969. Nuclear chemistry. 1970. 39 p. Sw. cr. 10:--.
398. Prompt gamma radiation from fragments in the thermal fission of ^{235}U . By H. Albinsson and L. Lindow. 1970. 48 p. Sw. cr. 10:--.
399. Analysis of pulsed source experiments performed in copper-reflected fast assemblies. By J. Kockum. 1970. 32 p. Sw. cr. 10:--.
400. Table of half-lives for excited nuclear levels. By S. G. Malmkog. 1970. 33 p. Sw. cr. 10:--.
401. Needle type solid state detectors for in vivo measurement of tracer activity. By A. Lauber, M. Wolgast. 1970. 43 p. Sw. cr. 10:--.
402. Application of pseudo-random signals to the Ågesta nuclear power station. By P.-Å. Bliselius. 1970. 30 p. Sw. cr. 10:--.
403. Studies of redox equilibria at elevated temperatures 2. An automatic divided-function autoclave and cell with flowing liquid junction for electrochemical measurements on aqueous systems. By K. Johnsson, D. Lewis and M. de Pourbaix. 1970. 38 p. Sw. cr. 10:--.
404. Reduction of noise in closed loop servo systems. By K. Nygaard. 1970. 23 p. Sw. cr. 10:--.
405. Spectral parameters in water-moderated lattices. A survey of experimental data with the aid of two-group formulae. By E. K. Sokolowski. 1970. 22 p. Sw. cr. 10:--.
406. The decay of optically thick helium plasmas, taking into account ionizing collisions between metastable atoms or molecules. By J. Stevetelt. 1970. 18 p. Sw. cr. 10:--.
407. Zooplankton from Lake Mägelungen, Central Sweden 1960-63. By E. Almqvist. 1970. 62 p. Sw. cr. 10:--.
408. A method for calculating the washout of elemental iodine by water sprays. By E. Bachofner and R. Hesböl. 1970. 24 p. Sw. cr. 10:--.
409. X-ray powder diffraction with Guinier-Hägg focusing cameras. By A. Bröwn. 1970. 102 p. Sw. cr. 10:--.
410. General physic section Progress report. Fiscal year 1969/70. By J. Braun. 1970. 92 p. Sw. cr. 10:--.
411. In-pile determination of the thermal conductivity of UO_2 in the range 500-2500 degrees centigrade. By J.-Å. Gyllander. 1971. 70 p. Sw. cr. 10:--.
412. A study of the ring test for determination of transverse ductility of fuel element canning. By G. Anevi and G. Östberg. 1971. 17 p. Sw. cr. 15:--.
413. Pulse radiolysis of Aqueous Solutions of aniline and substituted anilines. By H. C. Christensen. 1971. 40 p. Sw. cr. 15:--.
414. Radiolysis of aqueous toluene solutions. By H. C. Christensen and R. Gustafson. 1971. 20 p. Sw. cr. 15:--.
415. The influence of powder characteristics on process and product parameters in UO_2 pelletization. By U. Rumpfors. 1971. 32 p. Sw. cr. 15:--.
416. Quantitative assay of Pu239 and Pu240 by neutron transmission measurements. By E. Johansson. 1971. 26 p. Sw. cr. 15:--.
417. Yield of prompt gamma radiation in slow-neutron induced fission of ^{235}U as a function of the total fragment kinetic energy. By H. Albinsson. 1971. 38 p. Sw. cr. 15:--.
418. Measurements of the spectral light emission from decaying high pressure helium plasmas. By J. Stevetelt and J. Johansson. 1971. 48 p. Sw. cr. 15:--.
419. Progress report 1970. Nuclear chemistry. 1971. 32 p. Sw. cr. 15:--.
420. Energies and yields of prompt gamma rays from fragments in slow-neutron induced fission of ^{235}U . By H. Albinsson. 1971. 56 p. Sw. cr. 15:--.
421. Decay curves and half-lives of gamma-emitting states from a study of prompt fission gamma radiation. By H. Albinsson. 1971. 28 p. Sw. cr. 15:--.
422. Adjustment of neutron cross section data by a least square fit of calculated quantities to experimental results. Part 1. Theory. By H. Häggblom. 1971. 28 p. Sw. cr. 15:--.
423. Personnel dosimetry at AB Atomenergi during 1969. By J. Carlsson and T. Wahlberg. 1971. 10 p. Sw. cr. 15:--.
424. Some elements of equilibrium diagrams for systems of iron with water above 100°C and with simple chloride, carbonate and sulfate melts. By D. Lewis. 1971. 40 p. Sw. cr. 15:--.
425. A study of material buckling in uranium-loaded assemblies of the fast reactor FR0. By R. Håkansson and L. I. Tirén. 1971. 32 p. Sw. cr. 15:--.
426. Dislocation line tensions in the noble metals, the alkali metals and β -Brass. By B. Pettersson and K. Malén. 1971. 14 p. Sw. cr. 15:--.
427. Studies of fine structure in the flux distribution due to the heterogeneity in some FR0 cores. By T. L. Andersson and H. Häggblom. 1971. 32 p. Sw. cr. 15:--.
428. Integral measurement of fission-product reactivity worths in some fast reactor spectra. By T. L. Andersson. 1971. 36 p. Sw. cr. 15:--.
429. Neutron energy spectra from neutron induced fission of ^{235}U at 0.95 MeV and of ^{238}U at 1.35 and 2.02 MeV. By E. Almén, B. Holmqvist and T. Wiedling. 1971. 16 p. Sw. cr. 15:--.
430. Optical model analyses of experimental fast neutron elastic scattering data. By B. Holmqvist and T. Wiedling. 1971. 238 p. Sw. cr. 20:--.
431. Theoretical studies of aqueous systems above 25°C. 1. Fundamental concepts for equilibrium diagrams and some general features of the water system. By Derek Lewis. 1971. 27 p. Sw. cr. 15:--.
432. Theoretical studies of aqueous systems above 25°C. 2. The iron - water system. By Derek Lewis. 1971. 41 p. Sw. cr. 15:--.
433. A detector for (n, γ) cross section measurements. By J. Hellström and S. Beshai. 1971. 22 p. Sw. cr. 15:--.
434. Influence of elastic anisotropy on extended dislocation nodes. By B. Pettersson. 1971. 27 p. Sw. cr. 15:--.
435. Lattice dynamics of CsBr. By S. Rolandson and G. Raunio. 1971. 24 p. Sw. cr. 15:--.
436. The hydrolysis of iron (III) and iron (II) ions between 25°C and 375°C. By Derek Lewis. 1971. 16 p. Sw. cr. 15:--.
437. Studies of the tendency of intergranular corrosion cracking of austenitic Fe-Cr-Ni alloys in high purity water at 300°C. By W. Hübner, B. Johansson and M. de Pourbaix. 1971. 30 p. Sw. cr. 15:--.
438. Studies concerning water-surface deposits in recovery boilers. By O. Strandberg, J. Arvesen and L. Dahl. 1971. 132 p. Sw. cr. 15:--.
439. Adjustment of neutron cross section data by a least square fit of calculated quantities to experimental results. Part II. Numerical results. By H. Häggblom. 1971. 70 p. Sw. cr. 15:--.
440. Self-powered neutron and gamma detectors for in-core measurements. By O. Strindehag. 1971. 16 p. Sw. cr. 15:--.
441. Neutron capture gamma ray cross sections for Ta, Ag, In and Au between 30 and 175 keV. By J. Hellström and S. Beshai. 1971. 30 p. Sw. cr. 15:--.
442. Thermodynamical properties of the solidified rare gases. By I. Ebbsjö. 1971. 46 p. Sw. cr. 15:--.
443. Fast neutron radiative capture cross sections for some important standards from 30 keV to 1.5 MeV. By J. Hellström. 1971. 22 p. Sw. cr. 15:--.
444. A Ge (Li) bore hole probe for in situ gamma ray spectrometry. By A. Lauber and O. Landström. 1971. 26 p. Sw. cr. 15:--.
445. Neutron inelastic scattering study of liquid argon. By K. Sköld, J. M. Rowe, G. Ostrowski and P. D. Randolph. 1972. 62 p. Sw. cr. 15:--.
446. Personnel dosimetry at Studsvik during 1970. By L. Hedlin and C.-O. Widell. 1972. 8 p. Sw. cr. 15:--.
447. On the action of a rotating magnetic field on a conducting liquid. By E. Dahlberg. 1972. 60 p. Sw. cr. 15:--.
448. Low grade heat from thermal electricity production. Quantity, worth and possible utilisation in Sweden. By J. Christensen. 1972. 102 p. Sw. cr. 15:--.
449. Personnel dosimetry at studsvik during 1971. By L. Hedlin and C.-O. Widell. 1972. 8 p. Sw. cr. 15:--.
450. Deposition of aerosol particles in electrically charged membrane filters. By L. Ström. 1972. 60 p. Sw. cr. 15:--.
451. Depth distribution studies of carbon in steel surfaces by means of charged particle activation analysis with an account of heat and diffusion effects in the sample. By D. Brune, J. Lorenzen and E. Vitalis. 1972. 46 p. Sw. cr. 15:--.
452. Fast neutron elastic scattering experiments. By M. Salama. 1972. 98 p. Sw. cr. 15:--.
453. Progress report 1971. Nuclear chemistry. 1972. 21 p. Sw. cr. 15:--.
454. Measurement of bone mineral content using radiation sources. An annotated bibliography. By P. Schmeling. 1972. 64 p. Sw. cr. 15:--.
455. Long-term test of self-powered detectors in HBWR. By M. Brakas, O. Strindehag and B. Söderlund. 24 p. 1972. Sw. cr. 15:--.
456. Measurement of the effective delayed neutron fraction in three different FR0-cores. By L. Moberg and J. Kockum. 1972. Sw. cr. 15:--.
457. Applications of magnetohydrodynamics in the metal industry. By T. Robinson, J. Braun and S. Linder. 1972. 42 p. Sw. cr. 15:--.
458. Accuracy and precision studies of a radiochemical multielement method for activation analysis in the field of life sciences. By K. Samsahl. 1972. 20 p. Sw. cr. 15:--.
459. Temperature increments from deposits on heat transfer surfaces: the thermal resistivity and thermal conductivity of deposits of magnetite, calcium hydroxy apatite, humus and copper oxides. By T. Kelén and J. Arvesen. 1972. 68 p. Sw. cr. 15:--.
460. Ionization of a high-pressure gas flow in a longitudinal discharge. By S. Palmgren. 1972. 20 p. Sw. cr. 15:--.
461. The caustic stress corrosion cracking of alloyed steels - an electrochemical study. By L. Dahl, T. Dahlgren and N. Lagmyr. 1972. 43 p. Sw. cr. 15:--.
462. Electrodeposition of "point" Cu^{129}I roentgen sources. By P. Beronius, B. Johansson and R. Söremark. 1972. 12 p. Sw. cr. 15:--.
463. A twin large-area proportional flow counter for the assay of plutonium in human lungs. By R. C. Sharma, I. Nilsson and L. Lindgren. 1972. 50 p. Sw. cr. 15:--.
464. Measurements and analysis of gamma heating in the R2 core. By R. Carlsson and L. G. Larsson. 1972. 34 p. Sw. cr. 15:--.
465. Determination of oxygen in zircaloy surfaces by means of charged particle activation analysis. By J. Lorenzen and D. Brune. 1972. 18 p. Sw. cr. 15:--.

List of published AES-reports (In Swedish)

1. Analysis by means of gamma spectrometry. By D. Brune. 1961. 10 p. Sw. cr. 6:--.
 2. Irradiation changes and neutron atmosphere in reactor pressure vessels - some points of view. By M. Grounes. 1962. 33 p. Sw. cr. 6:--.
 3. Study of the elongation limit in mild steel. By G. Östberg and R. Attermo. 1963. 17 p. Sw. cr. 6:--.
 4. Technical purchasing in the reactor field. By Erik Jonson. 1963. 64 p. Sw. cr. 8:--.
 5. Ågesta nuclear power station. Summary of technical data, descriptions, etc. for the reactor. By B. Lilliehöök. 1964. 336 p. Sw. cr. 15:--.
 6. Atom Day 1965. Summary of lectures and discussions. By S. Sandström. 1966. 321 p. Sw. cr. 15:--.
 7. Building materials containing radium considered from the radiation protection point of view. By Stig O. W. Bergström and Tor Wahlberg. 1967. 26 p. Sw. cr. 10:--.
 8. Uranium market. 1971. 30 p. Sw. cr. 15:--.
 9. Radiography day at Studsvik. Tuesday 27 april 1971. Arranged by AB Atomenergi, IVA's Committee for nondestructive testing and TRC AB. 1971. 102 p. Sw. cr. 15:--.
 10. The supply of enriched uranium. By M. Mårtensson. 1972. 53 p. Sw. cr. 15:--.
- Additional copies available from the Library of AB Atomenergi, Fack, S-611 01 Nyköping 1, Sweden.